Journal of Hydrology 614 (2022) 128544

Contents lists available at ScienceDirect

Journal of Hydrology

journal homepage: www.elsevier.com/locate/jhydrol

Research papers

Development and testing of a dynamic CO_2 input method in SWAT for simulating long-term climate change impacts across various climatic locations

Yingqi Zhang [a,b], Junyu Qi [c], Dongmei Pan [a,b], Gary W. Marek [d], Xueliang Zhang [a,b], Puyu Feng [a,b], Haipeng Liu [a], Baogui Li [a,b], Beibei Ding [a,b], David K. Brauer [d], Raghavan Srinivasan [e], Yong Chen [a,b,*]

[a] College of Land Science and Technology, China Agricultural University, No. 2 Yuanmingyuan W Rd, Haidian District, Beijing 100193, China
[b] Key Laboratory of Arable Land Conservation in North China, Ministry of Agriculture and Rural Affairs, Beijing 100193, China
[c] Earth System Science Interdisciplinary Center, University of Maryland, College Park, MD 20740, USA
[d] USDA-ARS Conservation and Production Research Laboratory, 300 Simmons Rd., Unit 10, Bushland, TX 79012, USA
[e] Department of Ecosystem Science and Management, Texas A&M University, 2138 TAMU, College Station, TX 77843, USA

ARTICLE INFO

Keywords:
Hydrological modeling
SWAT-CO_2
Global climate change
General Circulation Models (GCMs)
Irrigated agriculture
U.S. High Plains

ABSTRACT

Water resources in semi-arid and arid regions are critical for sustainable agricultural development, and climate change imposes great challenges and brings about large uncertainties in water resource management and crop production. In this study, the effects of future climate change on hydrology and corn production in the U.S. High Plains region were assessed using a newly developed SWAT-CO_2 model and GCMs under the RCP4.5 and 8.5 scenarios. Specifically, a new method to dynamically input annual CO_2 concentration into SWAT was developed. This method, along with the SWAT default CO_2 concentration (330 ppm), and a constant CO_2 input option (one average CO_2 concentration for a simulation period) were compared for simulating hydrology and corn yield in 21st century (2031–2100). Results showed the default CO_2 concentration continuously simulated the highest crop evapotranspiration (ET_c) and irrigation but the lowest water yield and corn yield among three methods, especially under the RCP8.5 scenario. However, the ET_c and irrigation were higher for the dynamic input method before the mid-21st century and lower between mid- to late-21st century than for the constant input method. The contrast results were found for the corn yield simulations. Additionally, the improved SWAT-CO_2 model was applied to predict the changes in hydrology and corn yields for three centuries (2031–2298) relative to the historical period (1970–1999). Results indicated that the overall trend of future irrigation, ET_c, and corn yield could decrease significantly at the three sites compared to the historical period. The impacts of dramatically elevated CO_2 and logarithmic increase in air temperatures were the key factors for the above changes. The study highlighted the necessity of considering the dynamic CO_2 input for the SWAT applications in climate change studies. Long-term projected results of this study can inform local producers about the risks of future climate change in this water shortage environment.

1. Introduction

The rapid development of modern societies, along with an increased global population and economy have been fueled by a steady increase in the burning of fossil fuels for decades. As a result, climatic change has emerged due to the rising concentrations of greenhouse gases. The most visible evidence of climate change is rising air temperatures which are closely associated with changes in the global water cycle (El-Shehawy et al., 2012). The 2015 Paris Agreement on Climate Change committed to limiting global average temperature increases to <2 °C, and pursuing efforts to achieve temperature increases of <1.5 °C above pre-industrial levels (United Nations Framework Convention on Climate, 2015). This agreement attempts to mitigate the overall impacts of climate change and reduce the occurrence of extreme events (Lewis et al., 2019). Therefore, assessing the potential impacts of future climate change provide an invaluable and essential contribution to achieving carbon

* Corresponding author.
E-mail address: yongchen@cau.edu.cn (Y. Chen).

https://doi.org/10.1016/j.jhydrol.2022.128544
Received 3 August 2022; Received in revised form 13 September 2022; Accepted 30 September 2022
Available online 19 October 2022

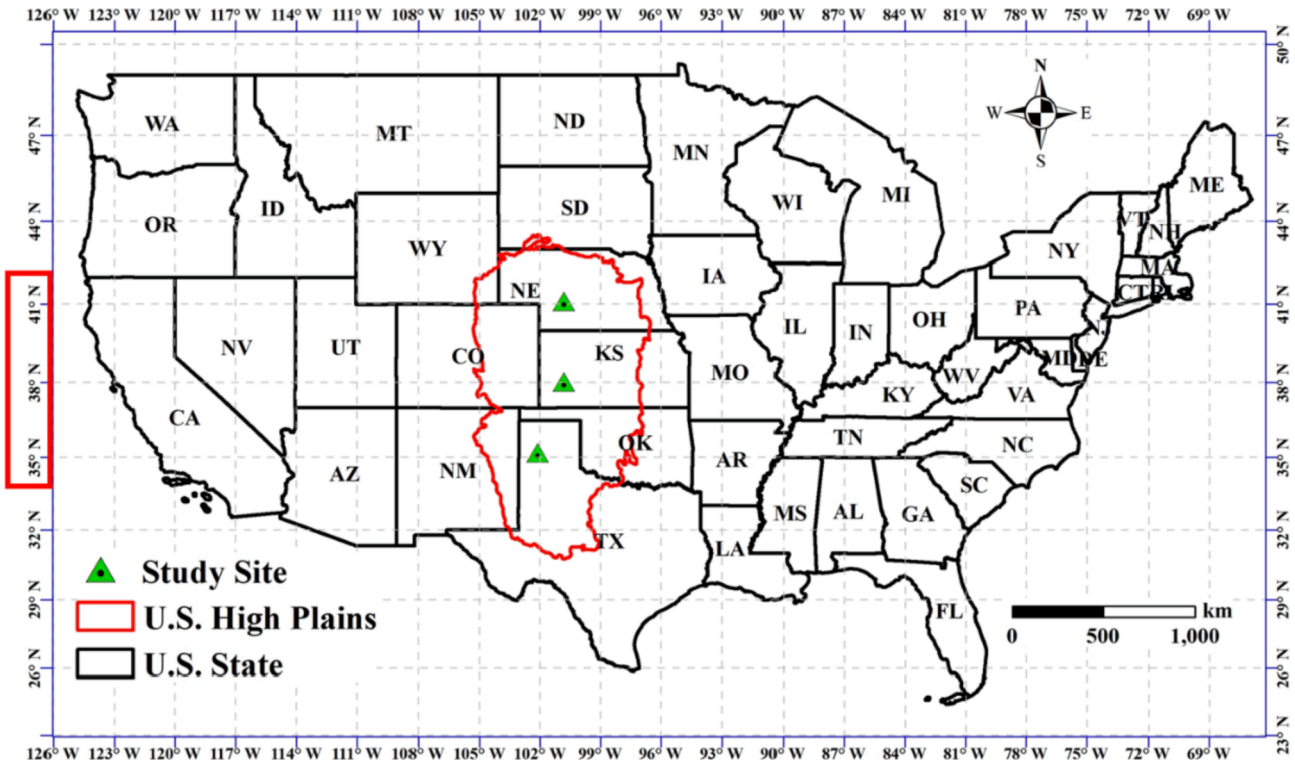

Fig. 1. Locations of the U.S. High Plains and the three study sites.

emission reductions for reducing global temperatures and associated negative impacts for the world (Qian et al., 2021).

Simulation modeling has shown that climate change can have great impacts on hydrology and crop yields (Chen et al., 2021). For instance, it is predicted that by the end of 21st century, climate change may result in a 16.3% reduction in global water use efficiency under a high emission scenario and a 2.2% reduction under a low emission scenario (Pan et al., 2018). Agriculture and climate change are inseparably linked, and agricultural systems are vulnerable to the impacts of climate change. Factors related to agricultural production such as CO_2 concentration, air temperature, precipitation, solar radiation, and other factors are affected by climate change (Feng et al., 2021; Marras et al., 2021). Therefore, global climate change is widely recognized as one of the most significant challenges faced by agriculture today. It is necessary to explore the impact of climate change on the hydrologic cycle and crop production, particularly across various climatic regions.

Climate projections from the IPCC Fifth Assessment Report (AR5) were based on the fifth phase of the Coupled Model Intercomparison Project (CMIP5), which focused on Representative Concentration Pathways (RCPs) for future climate projections by various General Circulation Models (GCMs) (Rogelj et al., 2012; Sheffield et al., 2013). The GCM outputs of CMIP5 have been widely used to study climate change related scenarios at regional and global scales (Zhang et al., 2019). Thus, CMIP5 projections could provide a good basis for the assessment of hydrological variables and crop growth parameters (Yuan et al., 2020). The use of the watershed-scale Soil and Water Assessment Tool (SWAT) facilitates the study of the impact of climate change on the regional water balance and crop production (Tan et al., 2022; Wang et al., 2020).

Water resources are limited in the southwest United States (U.S.), and irrigated agriculture is a major economic contributor to the U.S. High Plains region, which relies heavily on the Ogallala Aquifer as an irrigation source (Rudnick et al., 2019). Corn (*Zea mays* L.) is one of the major field crops planted under irrigated conditions in the U.S. High Plains (National Agricultural Statistics Service; NASS, 2021). Therefore, three corn production sites in the U.S. High Plains were selected for climate change evaluation in this study, including fields in Nebraska, Kansas, and Texas, ranging from north to south representing different regional climates.

The existing method for simulating CO_2 concentration in SWAT is problematic in that it only allows for a static input value for CO_2 concentration that remains constant for the entire simulation period, which has limitations for long-term future climate change simulations. In this study, a dynamic CO_2 input method was developed to allow for varying annual CO_2 values in the SWAT model. This development is both more flexible and realistic for long-term continuous simulations and essential for assessing future climate change on water balance and crop growth (Tan et al., 2020; Wang et al., 2017). Such an approach is also more convenient and computationally efficient than splitting long-term simulations into numerous, smaller simulation scenarios. It also likely allows for prediction results to be more representative and accurate. In addition, the previous studies of climate change lack long-term simulations, such as those from 2031 to 2300. In this study, climate data from four GCMs and two RCP scenarios (RCP4.5 and RCP8.5) based on the CMIP5 for three sites, Nebraska, Kansas, and Texas in the U.S. High Plains, were used to drive an improved SWAT model with the management allowed depletion (MAD) auto-irrigation algorithm and dynamic CO_2 input method. An assessment was undertaken to determine the impact of projected future climate change on hydrology and corn yields in the U.S. High Plains. Specifically, the objectives of this study were to (1) develop a new method for dynamically inputting CO_2 annual concentrations into the SWAT model; (2) compare the differences in the effects of three CO_2 input methods (SWAT default CO_2 input – 330 ppm, constant CO_2 input – one average value, and dynamic CO_2 input) on the hydrologic cycle and corn yields in the U.S. High Plains during 2031 to 2100; and (3) assess the long-term impacts of climate change on hydrology and corn yields across the U.S. High Plains from 2031 to 2298 using the newly developed dynamic CO_2 input method compared with the historical period (1970–1999).

Table 1
Descriptions of the future climate change scenarios.

Periods		Emission scenario*	CO_2 concentration (ppm)
2031–2100**		RCP4.5 and 8.5	Default CO_2 Input (330)
		RCP4.5	Constant CO_2 Input (506)
		RCP8.5	Constant CO_2 Input (661)
		RCP4.5 and 8.5	Dynamic CO_2 Input
Historical period (1970–1999)		–	Dynamic CO_2 Input
Future periods	2031–2060	RCP4.5 and 8.5	Dynamic CO_2 Input
	2061–2090		
	2091–2120		
	2121–2150		
	2151–2180		
	2181–2210		
	2211–2240		
	2241–2270		
	2271–2298		
	2031–2298		

* RCP: Representative Concentration Pathway.
** Five years of data (2026–2030) were used for the SWAT model warm up.

2. Materials and methods

2.1. Study sites

Three field study sites located in the U.S. High Plains were chosen for use in this study. Their locations were North Platte, Nebraska (41.2°N, 100.9°W, approximately 861 m above sea level); Garden City, Kansas (38.0°N, 100.8°W, approximately 887 m); and Bushland, Texas (35.2°N, 102.1°W, approximately 1171 m) (Fig. 1). All three study sites are classified as having a semi-arid climate (Peel et al., 2007) although air temperature and rainfall regimes vary. The U.S. High Plains area is the most important region for irrigated corn production in the nation. The average annual precipitation for the Nebraska site was ~506 mm. The mean annual maximum air temperature was ~17.3°C and the minimum air temperature was ~2.8°C. The soil type at the Nebraska site was classified as Cozad silt loam (Soil Survey Staff, 2010). The Kansas site had an average annual precipitation of ~439 mm, an average annual maximum air temperature of 21.2°C, and a minimum air temperature of 4.3°C. The soil type was Ulysses silt loam at the Kansas site. For the Texas site, the average annual precipitation was less than those for Nebraska and Kansas, at ~346 mm, with average annual maximum and minimum air temperatures of 22.3°C and 3.7°C, respectively. The soil type at the Texas site was Pullman silt clay loam.

2.2. CMIP5 future climate data

The CMIP5 future climate data used in this study were downloaded from the C3S Climate Data Store (https://cds.climate.copernicus.eu/cdsapp#!/dataset/projections-cmip5-daily-single-levels?tab=form). Only four GCMs were available with climate projection up to year 2300 for both RCP4.5 and RCP8.5 scenarios, namely CCSM4 (NCAR, USA), CSIRO-MK3-6-0 (CSIRO, Australia), IPSL-CM5A-LR (IPSL, France), and MPL-ESM-LR (MPI, Germany). The RCP4.5 scenario was a medium forcing scenario, which had a stable radiative forcing of 4.5 W m^{-2} by 2100, and the RCP8.5 scenario was a high forcing scenario, which had a stable radiative forcing of 8.5 W m^{-2} by 2100 (van Vuuren et al., 2011).

2.3. SWAT, SWAT-MAD, and SWAT- CO_2 models

2.3.1. SWAT model

The SWAT model is a continuous-time, semi-distributed, process-based, watershed-scale model (Arnold et al., 2012). It is a physically based hydrologic model that simulates crop growth, hydrology, and water quality. Its primary model components include a weather simulator, hydrology, plant growth, and land management, as well as loads and fluxes of sediment, nutrients, pesticides, bacteria, and pathogens. The SWAT model is described in detail by Neitsch et al. (2011). The SWAT2012 revision 664 was used in this study.

The SWAT model simulates hydrological processes in the soil profile based on the water balance equation [Eq. (1)], including precipitation, irrigation, surface runoff, evapotranspiration, lateral flow, and percolation (Arnold et al., 1998; Neitsch et al., 2011):

$$SWt = SWo + \sum_{i=1}^{n}(Rday + Iday - Qsurf - ETa - Qlat - Wseep) \quad (1)$$

where SW_t is the final soil water content (mm); SW_o is the initial soil water content (mm); t is the time step (day); R_{day} is the amount of precipitation on day i (or snowmelt; mm); I_{day} is the amount of irrigation on day i (mm); Q_{surf} is the amount of surface runoff on day i (mm); ET_a is the amount of actual evapotranspiration on day i (mm); Q_{lat} is the amount of lateral flow on day i (mm); and W_{seep} is the amount of percolation on day i (mm).

The surface runoff is determined by a modified Soil Conservation Service (SCS) curve number method (Mishra and Singh, 2013). A kinematic storage model is used to calculate lateral flow (Sloan and Moore, 1984). A "tipping-bucket" algorithm is used to simulate soil water flow (Arnold et al., 2011; Neitsch et al., 2011). Percolating water from the lowest soil layer enters the vadose zone and is ultimately recharged to the aquifer. Evapotranspiration for the SWAT model can be calculated by three different methods, which include the Penman-Monteith method (Monteith, 1965), the Priestley-Taylor method (Priestley and Taylor, 1972), and the Hargreaves method (Hargreaves and Samani, 1985). The Penman-Monteith method was used to simulate evapotranspiration in this study.

Plant growth was modulated using heat unit theory according to plant-specific input parameters, which were summarized in the plant growth database (Neitsch et al., 2011). SWAT first calculates potential growth using a leaf area index (LAI) function, determined by accumulated heat units, light interception, and converted intercepted light into biomass through radiation use efficiency. Actual growth is then calculated from the potential growth attributed to stresses, such as extreme temperatures and deficiencies of water and nutrients (i.e., nitrogen and phosphorus). Finally, SWAT calculates crop yield as a portion of total biomass using harvest index and partitions a part of dry crop biomass as

Table 2
SWAT model performance statistics in Texas, Kansas, and Nebraska sites.

Site (Year)	Calibrated variable	Nash-Sutcliffe efficiency (*NSE*)	Coefficient of determination (R^2)	Percent bias (*PBIAS*)
Texas (2013 and 2016)	Monthly irrigation	0.81	0.83	0.4 %
	Daily evapotranspiration	0.75	0.81	−11.7 %
	Leaf area index (LAI)	0.86	0.88	5.9 %
	Aboveground biomass	0.84	0.86	−5.3 %
Kansas (2005–2012)	Monthly irrigation	0.7	0.71	−16.4 %
Nebraska (2003–2006)	Monthly irrigation	0.56	0.56	−3.9 %

Table 3
Ensemble means of four GCMs for changes in ET_c, irrigation, water yield, and corn yield using three CO_2 input methods from 2031 to 2100 in Nebraska, Kansas, and Texas sites.

Scenario/Site		Input Method	ET_c (mm)	Irrigation (mm)	Water Yield (mm)	Corn Yield (Mg ha^{-1})
RCP4.5	Nebraska	Default	539.47 ± 16.60a	22.59 ± 17.52a	154.40 ± 54.19b	6.93 ± 0.43b
		Constant	503.85 ± 14.76b	13.61 ± 13.52b	182.08 ± 57.08a	7.68 ± 0.49a
		Dynamic	503.84 ± 14.23b	13.61 ± 13.73b	182.04 ± 56.95a	7.67 ± 0.45a
	Kansas	Default	645.46 ± 24.53a	119.83 ± 43.19a	137.72 ± 54.86b	7.06 ± 0.49b
		Constant	607.13 ± 22.09b	100.33 ± 38.61b	157.77 ± 58.56a	7.94 ± 0.54a
		Dynamic	606.64 ± 21.26b	99.97 ± 37.68b	157.87 ± 58.22a	7.92 ± 0.47a
	Texas	Default	648.78 ± 25.47a	92.53 ± 51.62a	51.22 ± 39.64b	5.05 ± 0.42b
		Constant	602.26 ± 22.53b	64.68 ± 44.05b	69.59 ± 47.08a	6.52 ± 0.53a
		Dynamic	602.25 ± 22.05b	64.86 ± 43.67b	69.62 ± 47.05a	6.50 ± 0.42a
RCP8.5	Nebraska	Default	556.47 ± 29.49a	29.21 ± 24.92a	142.67 ± 50.15b	6.12 ± 0.88b
		Constant	478.34 ± 22.66b	9.43 ± 12.73b	203.61 ± 56.96a	7.02 ± 0.97a
		Dynamic	467.52 ± 35.38c	6.62 ± 10.05b	211.16 ± 72.10a	6.93 ± 0.9a
	Kansas	Default	667.65 ± 34.23a	136.53 ± 42.87a	115.86 ± 50.06b	6.20 ± 0.97b
		Constant	581.85 ± 30.42b	90.08 ± 32.47b	158.14 ± 58.51a	7.23 ± 1.12a
		Dynamic	569.81 ± 40.43c	82.1 ± 29.93b	162.15 ± 59.12a	7.12 ± 1.00a
	Texas	Default	663.32 ± 30.03a	109.95 ± 60.35a	53.29 ± 38.86b	4.35 ± 0.86b
		Constant	564.27 ± 23.24b	50.07 ± 40.07b	90.62 ± 53.13a	6.38 ± 1.22a
		Dynamic	554.35 ± 56.84b	44.27 ± 35.36b	93.32 ± 46.99a	6.19 ± 0.69a

Columns with the same alphabets indicated that the differences were not significant ($P > 0.05$); different alphabets (a, b, and c) indicated that the differences were significant ($P < 0.05$).

dry economic yield (Arnold et al., 2011).

CMIP5 future climate data including daily precipitation and maximum & minimum air temperatures were projected by four GCMs in this study. The WXGEN weather generator model (Sharpley and Williams, 1990), which was embedded in the SWAT model, was used to simulate future daily solar radiation, wind speed, and relative humidity. For this weather generator model, it was presumed that the signatures of solar radiation, wind speed, and relative humidity would remain consistent with current levels under different future scenarios, which meant that precipitation and air temperatures were the major contributors to future hydrology and crop growth.

2.3.2. SWAT management allowed depletion auto-irrigation (SWAT-MAD) model

In practice, producers are willing to allow a maximum percentage of plant available water depletion before irrigation is triggered. This concept is known as management allowed depletion (MAD), a common framework for irrigation scheduling as outlined by Merriam (1966). MAD irrigation management has been widely applied in semi-arid/arid regions including Texas, Kansas, and Nebraska in the U.S. (Callison, 2012; Evett et al., 2011; Payero et al., 2008). For most crop production, a 50% MAD value represents a reasonable overall value for avoiding apparent crop water stress (Callison, 2012; USDA-NRCS, 2017). As for water sensitive crops or heavily compacted soils, a smaller range of depletion may be needed (30%-50% MAD). A larger MAD value can be used (50%-70%) for stress-tolerant crops or well-structured soils. The current default auto-irrigation function in SWAT is unable to simulate MAD irrigation management explicitly. However, irrigation scheduling based on the MAD concept is becoming widely used (Marek et al., 2011; Evett et al., 2011). As a result, a MAD-based SWAT auto-irrigation algorithm is required for accurate simulation of actual irrigation operations. A MAD-based automatic irrigation algorithm based on a user-defined permissible percentage of plant available water depletion, determined by the maximum crop-specific root depth and soil properties, was developed for SWAT by Chen et al. (2018). MAD values approaching zero denote irrigation management frequencies that result in low plant water stress. Conversely, values approaching one result in irrigation management that leads to greater plant water stress, as expressed in Eq. (2).

$$(sol\_sumfc - sol\_sw) / PAW > MAD \quad (2)$$

where sol_sumfc is the amount of water held in the soil profile at field capacity (mm); sol_sw is the amount of water stored in soil profile on any given day (mm); PAW is plant available water, determined primarily by soil texture and plant-specific maximum rooting depth; and MAD is the management allowed depletion percentage (user-defined water stress threshold that triggers irrigation), expressed as a decimal value ranging from 0 to 1.

2.3.3. SWAT-CO_2 dynamic input method

CO_2 concentration is very important for SWAT model simulations. SWAT adjusts crop radiation use efficiency (RUE) according to different values of atmospheric CO_2 concentrations, so as to change both the conversion efficiency of crop photosynthesis and the accumulation of crop biomass. However, the SWAT default CO_2 concentration is set to 330 ppm. The default value can be changed by SWAT users but remains fixed at that value for the duration of the simulation. As such, different CO_2 concentrations cannot be assigned for different years within a single simulation which prevents simulation of increasing CO_2 concentrations over time in long-term simulations. This condition represents a critical deficiency in SWAT as CO_2 concentrations increase gradually over time under the RCP4.5 and 8.5 scenarios.

To overcome this problem, some scholars have modified the maximum stomatal conductance of crops to reflect the impact of CO_2 concentration changes on crops (Wu et al., 2012a, 2012b; Butcher et al., 2014); Chen et al. (2019) compensated for the low default CO_2 concentrations in future climate scenarios by dividing the simulation duration into multiple time periods and inputting the average CO_2 concentrations for the future climate simulation periods. Furthermore, some scholars modified the SWAT subroutine to output CO_2 and consider the dynamics of CO_2 emissions (Melaku et al., 2022; Qi et al., 2020). However, the above methods cannot fundamentally solve the problem of using dynamic CO_2 concentration in SWAT and associated

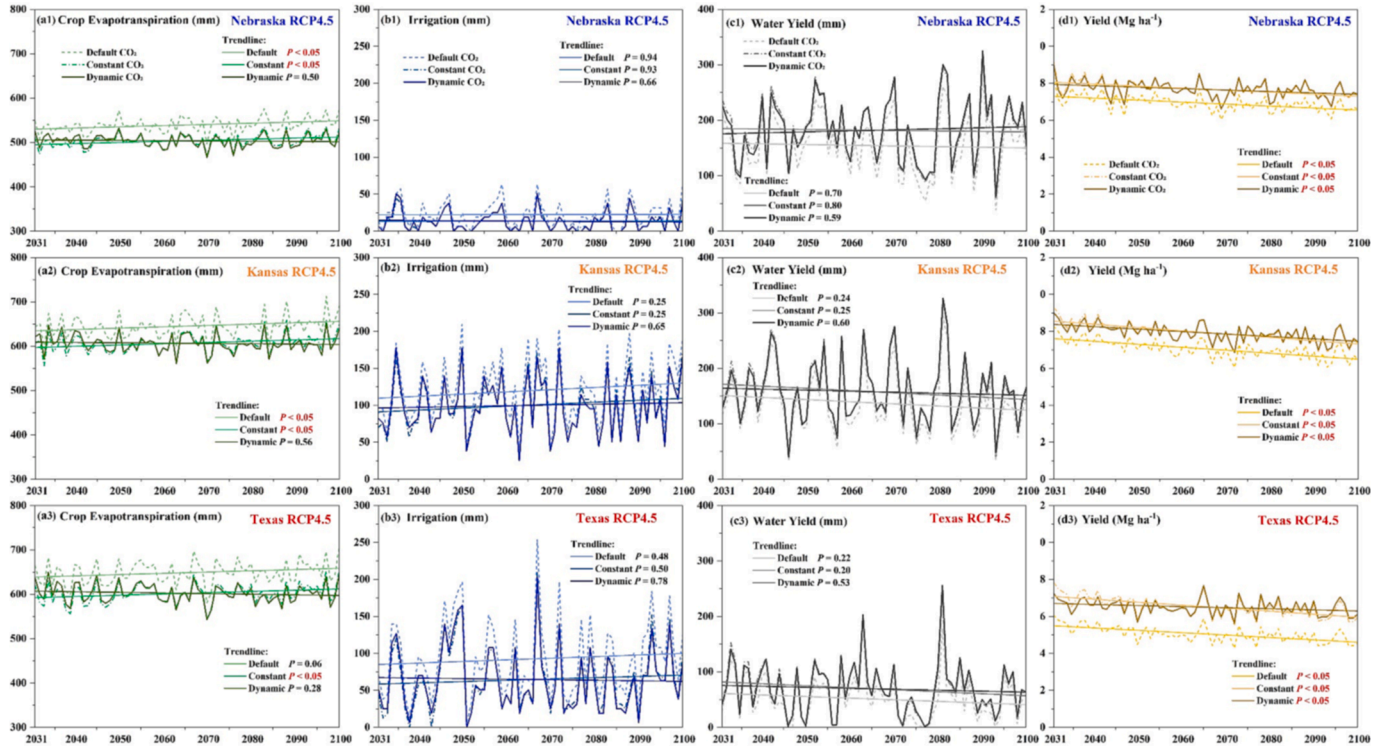

Fig. 2. Simulated future climate change impacts on irrigation, ET_c, water yield, and crop yields in three sites using three CO_2 input methods under RCP4.5 scenarios from 2031 to 2100 for the ensemble means of the four GCMs.

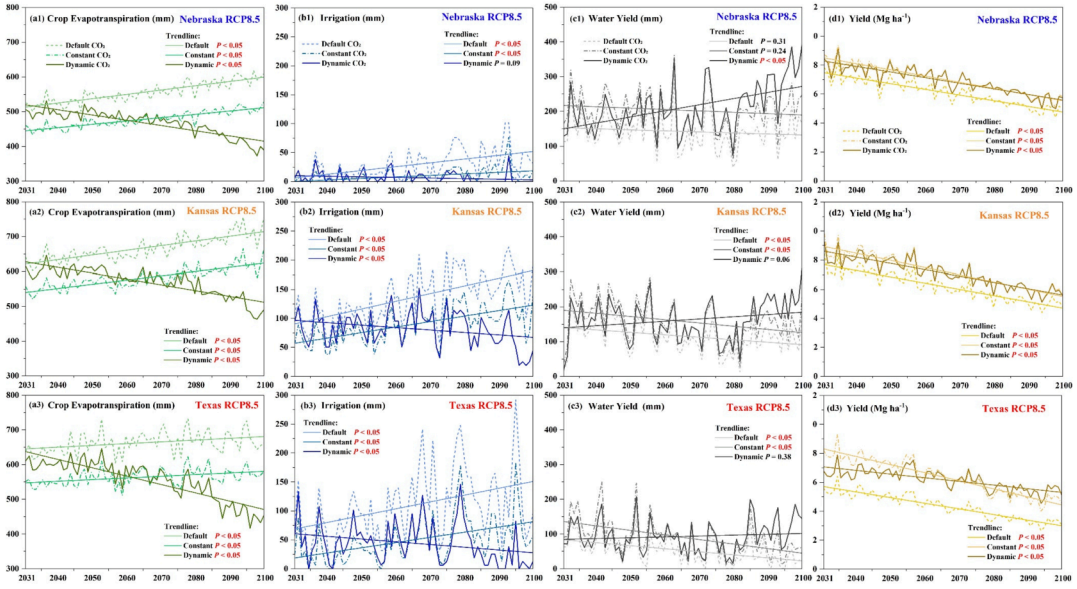

Fig. 3. Simulated future climate change impacts on irrigation, ET_c, water yield, and crop yields in three sites using three CO_2 input methods under RCP8.5 scenarios from 2031 to 2100 for the ensemble means of the four GCMs.

simulation results likely include intrinsic errors not easily discerned. Therefore, the development of dynamic CO_2 input method is both necessary and timely given current international interest in climate change simulation. In this study, a dynamic CO_2 input method was developed to incorporate projected IPCC annual CO_2 concentration data as input data for the SWAT model, thus allowing for simulations using changing annual CO_2 concentrations.

In this study, we created an input text file named "CO2con" with annual CO_2 concentrations derived from IPCC. A subroutine "readco2.f" was developed to read annual CO_2 concentration values in "CO2con" file for dynamic CO_2 simulations. Specifically, a global variable "co2con" was defined and used to receive the CO_2 concentration of current simulation year and then used in HRU level subroutines. The escalated CO_2 concentrations influenced the plant canopy resistance [Eqs. (3) and (4)], which further altered the potential evapotranspiration (PET) calculation. Furthermore, radiation use efficiency was also adjusted by elevated CO_2 concentrations [Eq. (5)], given as:

$$r_c = (0.5 * g_{l,co_2} * LAI)^{-1} \quad (3)$$

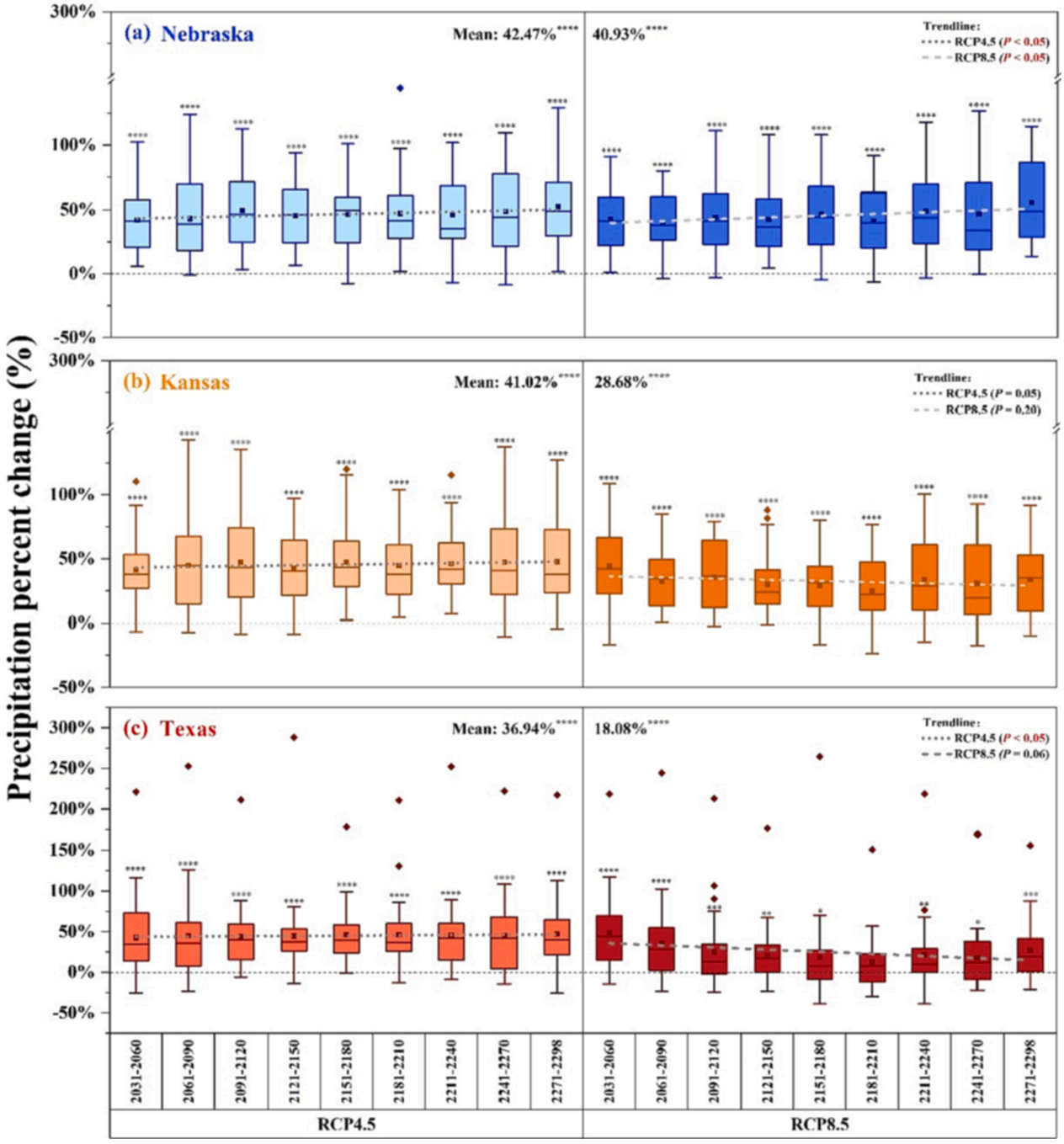

Fig. 4. Box plots showing the predicted annual percent changes in precipitation under RCP4.5 and RCP8.5 scenarios during the 2031–2060, 2061–2090, 2091–2120, 2121–2150, 2151–2180, 2181–2210, 2211–2240, 2241–2270, and 2271–2298 time periods compared to the historical period (1970–1999).

$$g_{l,co_2} = g_l * \left[1.4 - 0.4 * \left(\frac{CO_2}{330}\right)\right] \quad (4)$$

where r_c is the plant canopy resistance (m s^{-1}); g_l is the maximum conductance of a single leaf (m s^{-1}); *LAI* is the leaf area index of the canopy; g_{l,co_2} is the leaf conductance modified to reflect CO_2 effects (m s^{-1}); and CO_2 is the concentration of carbon dioxide in the atmosphere (ppm).

$$RUE = \frac{100 * CO_2}{CO_2 + \exp(r_1 - r_2 * CO_2)} \quad (5)$$

where *RUE* is the radiation use efficiency, which was defined as dry biomass generated for each unit of intercepted solar radiation (kg/ha·$(MJ/m^2)^{-1}$), and r_1 and r_2 are shape coefficients.

2.4. Model setup and evaluation

The daily meteorological data for Nebraska, Kansas, and Texas sites were obtained from the High Plains Regional Climate Center (HPRCC) weather network (https://hprcc.unl.edu/) including precipitation and maximum & minimum air temperatures. Measured hydrologic and agronomic data for the Texas site in 2013 and 2016 included lysimeter-measured daily crop evapotranspiration (ET_c), actual irrigation, LAI, and aboveground biomass for corn, whereas only actual irrigation data were collected for the Nebraska and Kansas sites (Chen et al., 2019a).

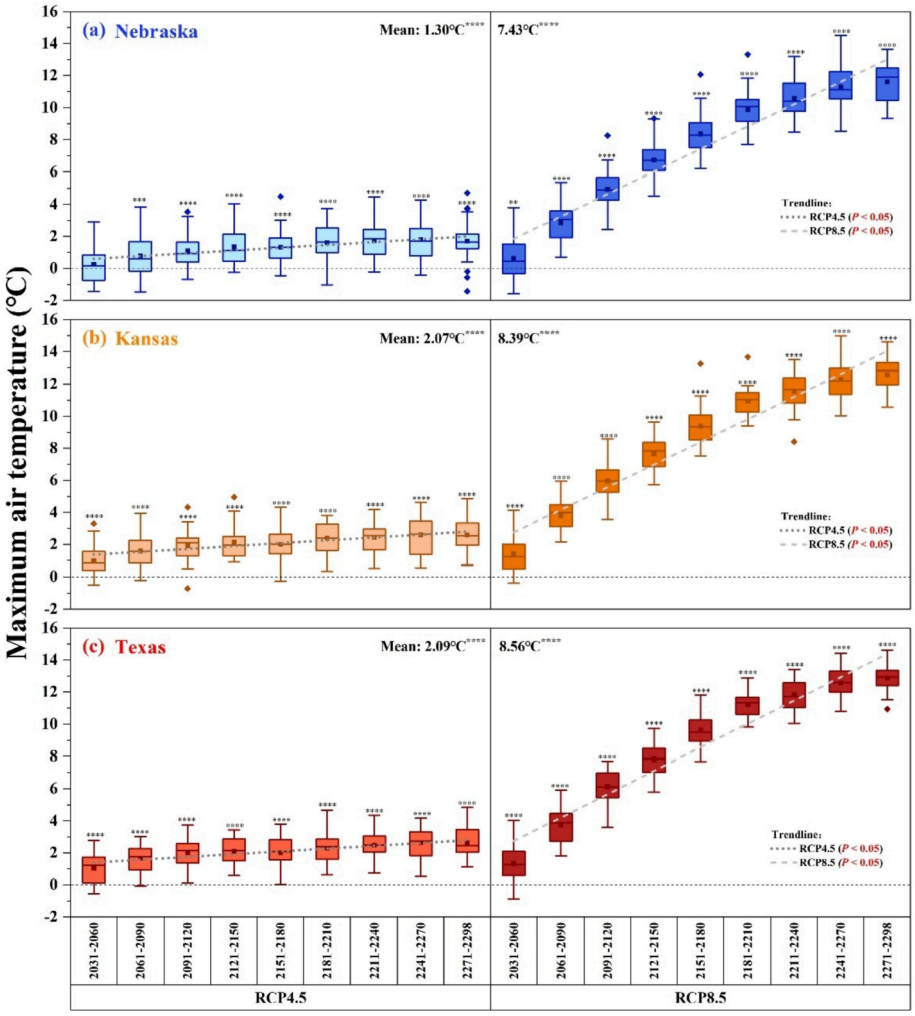

Fig. 5. Box plots showing the predicted annual percent changes in maximum air temperature under RCP4.5 and RCP8.5 scenarios during the 2031–2060, 2061–2090, 2091–2120, 2121–2150, 2151–2180, 2181–2210, 2211–2240, 2241–2270, and 2271–2298 time periods compared to the historical period (1970–1999).

The SWAT-MAD simulated irrigation was compared to actual irrigation at all three study sites for model evaluation.

Evaluation was performed at the hydrological response unit (HRU) level with measured daily ET_c, LAI, and aboveground biomass for Texas site. Evaluation of irrigation using the SWAT-MAD model was conducted for all three sites. The calibrated parameters for Texas from 2000 to 2010 were obtained from Chen et al. (2018), while Nebraska and Kansas sites used a parameter regionalization calibration method (Chen et al., 2019a). SWAT-MAD performance for simulated irrigation was analyzed using percent bias (*PBIAS*) (Gupta et al., 1999), coefficient of determination (R^2) (Legates and McCabe, 1999), and Nash-Sutcliffe efficiency (*NSE*) (Nash and Sutcliffe, 1970) statistics.

2.5. Scenario design

2.5.1. Three CO_2 input methods for 2031–2100

To better represent the impacts of CO_2 concentrations in model simulations of major hydrologic variables and crop yield under future climate change scenarios, three different methods for simulating CO_2 concentration were used: 1) the SWAT default value of 330 ppm, 2) a constant value of 506 or 661 ppm, calculated as the average concentration over the simulation period of 2031–2100 using the RCP4.5 and RCP8.5 scenarios, respectively, and 3) the dynamic CO_2 input method introduced in this study, which used different concentration values for each year (Table 1). These CO_2 concentration simulation approaches were termed the default input, constant input, and dynamic input methods.

2.5.2. Study periods (1970–1999 and 2031–2298)

The historical period of 1970–1999 was used as the baseline scenario. Future climate change simulations considered the RCP4.5 and RCP8.5 scenarios based on four GCMs from CMIP5. The future climate projections (2031–2298) were divided into nine 30-year periods: 2031–2060, 2061–2090, 2091–2120, 2121–2150, 2151–2180, 2181–2210, 2211–2240, 2241–2270, and 2271–2298. The first five years of data (e.g., 2026–2030) before the start of each period (e.g., 2031–2060) were used for the SWAT model warmup. The dynamic CO_2 input method was used in this long-term simulation (Table 1).

2.6. Statistical analysis

To compare the differences between the three CO_2 input methods from 2031 to 2100 for hydrology and corn yield at the three sites of Nebraska, Kansas, and Texas, the one-way ANOVA method was used to determine significant differences in the means of multiple samples under the influence of a single control variable. Samples having significant differences ($P < 0.05$) were indicated using letter designations (e.g., a, b, and c). In addition, a linear fit method was used to test the significance of the long-term trends for 2031–2100 and 2031–2298. The *t* test (Student's *t* test) was used to test the significance level for the ensemble

mean of four GCMs from 2031 to 2298 (i.e., nine 30-year time periods) with respect to the historical period. A nonparametric test, namely Wilcoxon's rank sum test (a rank-based reciprocity test) was used for data that were not normally distributed.

3. Results

3.1. Model performance evaluation

The model performance demonstrated satisfactory agreement between simulated and observed ET_c, LAI, and aboveground biomass for the Texas site. The *NSE*, R^2, and *PBIAS* values for daily ET_c were 0.75, 0.81, and −11.7% for the 2013 and 2016 simulation periods, respectively (Table 2). LAI matched well with observed data with *NSE*, R^2, and *PBIAS* values of 0.86, 0.88, and 5.9%, respectively. The simulated and observed values of aboveground biomass also agreed well with *NSE*, R^2, and *PBIAS* of 0.84, 0.86, and −5.3%, respectively (Table 2). The *NSE*, R^2, and *PBIAS* values for the SWAT-MAD simulated monthly irrigation amount at the Texas site were 0.81, 0.83, and 0.4%, respectively (Table 2). Compared to the actual irrigation amounts, the SWAT-MAD simulated monthly irrigation amounts for the Kansas site had *NSE*, R^2, and *PBIAS* values of 0.70, 0.71, and −16.4%, respectively, from 2005 to 2012. For the Nebraska site, the *NSE*, R^2, and *PBIAS* were 0.56, 0.56, and −3.9%, respectively, using the SWAT-MAD model for monthly irrigation amounts from 2003 to 2006 (Table 2). The results indicated a satisfactory model performance for all three sites.

3.2. Comparisons of simulated ET_c, irrigation, water yield, and corn yield using three CO_2 input methods

3.2.1. Difference in simulated ET_c

Under the RCP4.5 scenario, the default CO_2 input method simulated the greatest ET_c across locations from 2031 to 2100 ($P < 0.05$) while there was no significant difference in ET_c simulations using the constant and dynamic input methods across the three sites (Table 3). Furthermore, the default and constant input methods indicated a significant increasing trend in simulated ET_c from 2031 to 2100 under the RCP4.5 scenario (Fig. 2a1–a3), whereas the dynamic input method did not show a marked trend (Fig. 2a1–a3). It is worth noting that the margin of difference for the simulated ET_c between the default input method and the other two input methods tended to increase with the decreasing latitude at the three sites (Table 3; Fig. 2a1–a3).

Similar to the RCP4.5 scenario, the default method predicted the greatest ET_c among the three input methods under the RCP8.5 scenario (Table 3; Fig. 3a1–a3), and there was a significant increasing trend (greater slope than RCP4.5) for both the default and constant input methods from 2031 to 2100. Contrary to the RCP4.5 scenario, predicted ET_c for the dynamic input method showed a significant decreasing trend (Fig. 3a1–a3) while the simulated ET_c using the dynamic input method was greater than that of the constant input method before 2065 and less than that of the constant input after 2076. For the Nebraska and Kansas sites, the predicted average ET_c among the three methods all showed significant differences (Table 3). Similar to the RCP4.5 scenario, the difference in simulated ET_c among the three methods became more pronounced in the lower latitudes (Figs. 2 and 3).

3.2.2. Comparison of simulated irrigation

Similar to the ET_c results, the default CO_2 input method also simulated the greatest amount of irrigation relative to the other two input methods under the RCP4.5 scenario ($P < 0.05$) (Table 3; Fig. 2b1–b3). However, there were no significant differential trends over time using different input methods across the three sites (Fig. 2b1–b3). In general, the average irrigation was larger for the Kansas (ranging from 100.0 to 119.8 mm) and Texas (ranging from 64.7 to 92.5 mm) sites as compared to the Nebraska site (ranging from 13.6 to 22.6 mm) (Table 3). For the RCP8.5 scenario, predicted average irrigation using the default input method was significantly greater than values for the constant and dynamic input methods (Table 3). Moreover, predicted irrigation showed a significant upward trend from 2031 to 2100 under the default and constant input methods at all three sites, whereas there were significant decreasing trends for the Kansas and Texas sites using the dynamic input method (Fig. 3b1–b3).

3.2.3. Influence on water yield by three CO_2 input methods

Under the RCP4.5 scenario, the average annual water yield for the constant and dynamic input methods were significantly greater ($P < 0.05$) than the default input method (Table 3; Fig. 2c1–c3) across three sites (Table 3). No significant differential trend from 2031 to 2100 was found for predicted water yield using the three input methods across the three sites (Fig. 2c1–c3). Water yield decreased with decreasing latitude for all three CO_2 input methods (Table 3; Fig. 2c1–c3). Under the RCP8.5 scenario, average annual water yield simulated by the default input method remained significantly less than the other two methods across locations (Table 3). Unlike the RCP4.5 scenario, the trendline in water yield increased significantly using the dynamic method for the Nebraska site (Fig. 3c1), and for the Kansas and Texas sites, the trendlines decreased significantly with the default and constant input methods (Fig. 3c2 and c3).

3.2.4. Impact on corn yield using three input methods

The constant and dynamic input methods showed no significant difference for corn yield but their predictions were significantly greater ($P < 0.05$) than the default input method under the RCP4.5 scenario (Table 3; Fig. 2d1–d3). Furthermore, the trendlines for all three methods were significantly decreased at all sites (Fig. 2d1–d3), and the yield gap between the constant/dynamic input methods and the default input method increased with the decreasing latitudes. Under the RCP8.5 scenario, predicted average corn yields were lowest using the default input method (Table 3; Fig. 3d1–d3). Simulated yields using the dynamic input were less than those using the constant input in the first half of the study period (2031 to mid-21st century) for the Texas site and greater for those in the later part (late-mid 21st century to 2100) (Fig. 3d3). This can be explained by the CO_2 fertilizer effect when a dynamic increase in CO_2 concentration was simulated using the dynamic CO_2 input method. Predicted corn yield showed a significant declining trend for all three input methods across all three sites (Figs. 2 and 3d1-d3).

3.3. Projected future climate from 2031 to 2298

3.3.1. Projected precipitation

For all three sites, average annual precipitation increased significantly ($P < 0.05$) over nine 30-year periods from 2031 to 2298 as compared to the historical period (1970–1999) under both the RCP4.5 and 8.5 scenarios, except for 2081–2210 of RCP8.5 for the Texas site (Fig. 4). On average from 2031 to 2298, precipitation increased significantly by 42.5% and 40.9% for the RCP4.5 and 8.5 scenarios in the Nebraska site, 41.0% and 28.7% in the Kansas site, and 36.9% and 18.1% in the Texas site, respectively, compared to the historical period (Fig. 4). Simultaneously, there were significant increasing trends in the simulated precipitation over time for the Nebraska site in both RCP scenarios and for the Texas site using the RCP8.5 scenario (Fig. 4a and c). The precipitation anomalies were obviously increased for the Texas site, with the greatest percentage change anomaly of nearly 300 % between 2121 and 2150 for the RCP4.5 scenario (Fig. 4c).

3.3.2. Projected maximum and minimum air temperatures

Maximum and minimum air temperatures increased significantly ($P < 0.05$) over the nine 30-year periods compared to the historical period under the RCP4.5 and 8.5 scenarios in three sites (Fig. 5). Both maximum and minimum air temperatures showed significant increasing trends from 2031 to 2298 under both RCP scenarios with a logarithmic

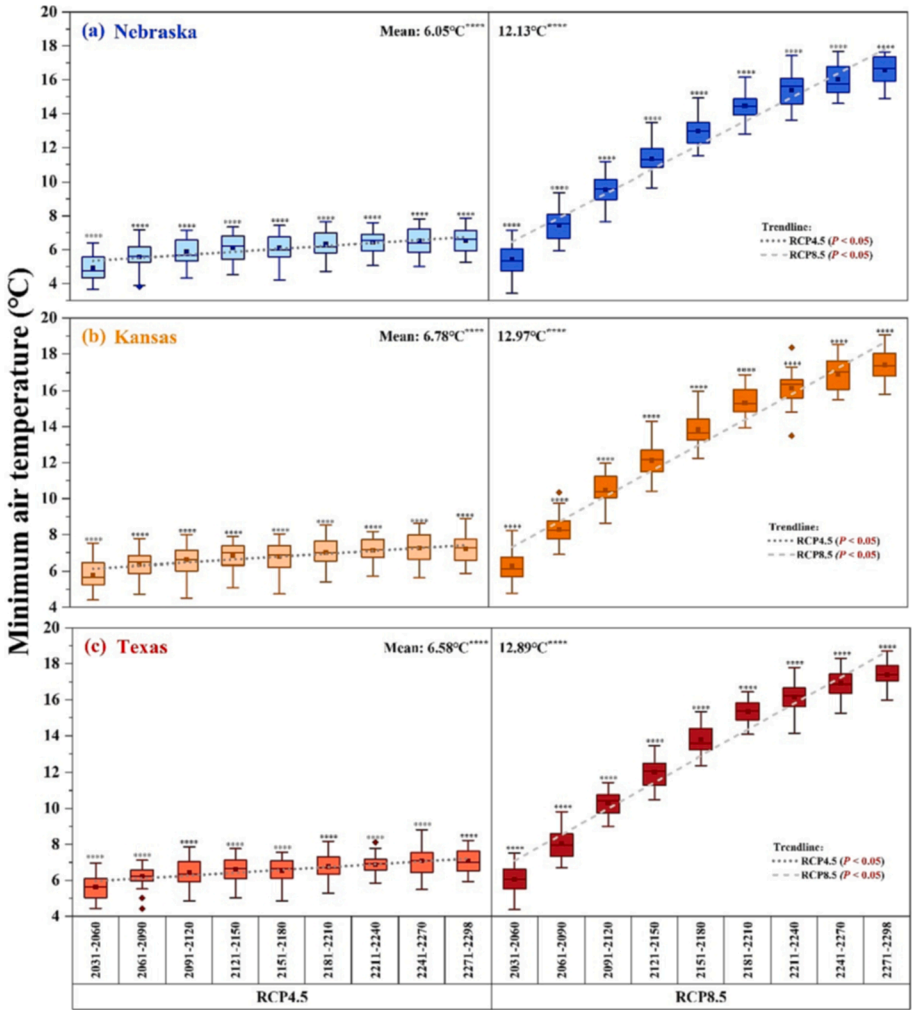

Fig. 6. Box plots showing the predicted annual percent changes in minimum air temperature under RCP4.5 and RCP8.5 scenarios during the 2031–2060, 2061–2090, 2091–2120, 2121–2150, 2151–2180, 2181–2210, 2211–2240, 2241–2270, and 2271–2298 time periods compared to the historical period (1970–1999).

form for the RCP8.5 scenario (Fig. 5). Under the RCP4.5 scenario, the mean values of maximum air temperature during the entire study period (2031–2298) increased by 1.30°C, 2.07°C, and 2.09°C relative to the historical period for the Nebraska, Kansas, and Texas sites, respectively. Under the RCP8.5 scenario, the average maximum air temperature increases were greater as compared to the RCP4.5 scenario, gradually increasing with decreasing latitude, with 7.43°C, 8.39°C, and 8.56°C from north to south for the three sites (Fig. 5).

It is worth noting that the increase in the minimum air temperature was much greater than that of the maximum air temperature (Fig. 6), with the entire period under the RCP4.5 scenario significantly increased by approximately 6°C (the average increases were 6.05°C, 6.78°C, and 6.58°C for the Nebraska, Kansas, and Texas sites). In addition, minimum air temperature increased significantly by approximately 5°C during the initial study period (2031–2060) and by approximately 17°C at the end of the 23rd century (2271–2298) for all three sites under the RCP8.5 scenario.

3.4. Long-term climate change impacts on ET_c, irrigation, water yield, and crop yield using the dynamic CO_2 input method for three centuries

3.4.1. Changes in ET_c

For the Nebraska site, ET_c was significantly less ($P < 0.05$) than the historical period from the 21st century to the first half of the 23rd century (2031 to 2240) under the RCP4.5 scenario (Fig. 7a) with an average decrease of 2.9% over the entire period (2031 to 2298). Although predicted ET_c was lower relative to the historical period for most 30-year periods, the trend increased significantly from 2031 to 2298. For the RCP8.5 scenario, ET_c was significantly lower than the historical period for all nine 30-year periods (Fig. 7a). The average percentage decrease in ET_c was 24.7% over the entire study period for the RCP8.5 scenario (Fig. 7a). For the Kansas site, a significant increase was found for ET_c from 2031 to 2060 and from 2121 to 2210 under the RCP4.5 scenario and a significant decrease for the periods of 2061–2298 were identified under the RCP8.5 scenario compared to the historical period. The mean values of percent change in ET_c were 2.5% and −19.0% for the RCP4.5 and 8.5 scenarios ($P < 0.05$). No significant differential trend of ET_c for the Kansas site was determined under either RCP scenario (Fig. 7b). For the Texas site, ET_c increased significantly from 2031 to 2120 and from 2241 to 2298 as compared to the historical period with a significant average increase of ~3.5% for the entire period under the RCP4.5 scenario. The average percent decrease in ET_c was approximately 24.0% from 2031 to 2298 ($P < 0.05$) with a significant declining trend over time under the RCP8.5 scenario (Fig. 7c).

3.4.2. Variations in irrigation

In general, average annual irrigation for most future periods was predicted to be less than that of the historical period under the RCP4.5 scenario with an average decrease of ~56.7%, 20.3%, and 56.7% from 2031 to 2298 for sites in Nebraska, Kansas, and Texas, respectively (Fig. 8). However, the trend in irrigation varied across the three sites with the Nebraska site having an increasing trend and the Texas site

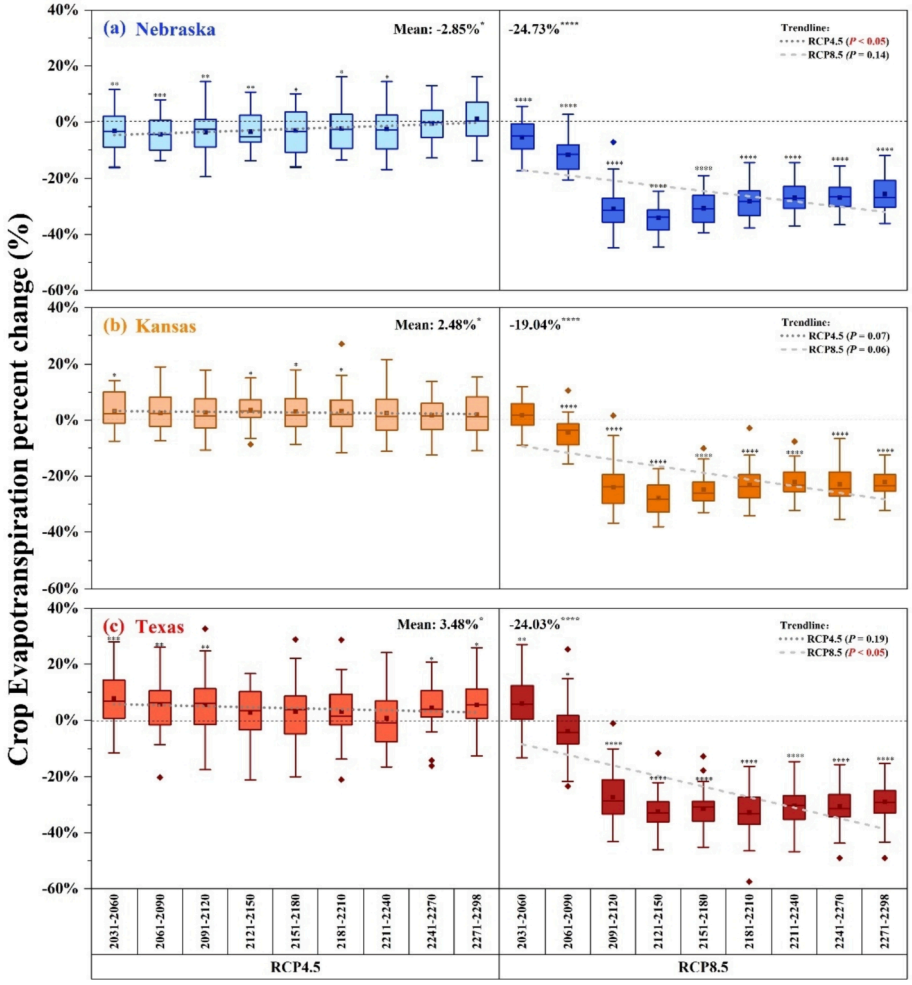

Fig. 7. Box plots showing the simulated annual percent changes in ET_c under RCP4.5 and RCP8.5 scenarios during the 2031–2060, 2061–2090, 2091–2120, 2121–2150, 2151–2180, 2181–2210, 2211–2240, 2241–2270, and 2271–2298 time periods compared to the historical period (1970–1999).

having a decreasing trend over time ($P < 0.05$). For the RCP8.5 scenario, predicted irrigation was significantly lower than the historical period with an average percentage decrease of ~96.0%, 63.9%, and 87.3% for sites in Nebraska, Kansas, and Texas, respectively, and all had a significant decreasing trend in irrigation (Fig. 8). Note that in the Nebraska and Texas sites, there was virtually no simulated irrigation between 2091 and 2298.

3.4.3. Water yield dynamics

For the Nebraska and Texas sites, water yield was significantly increased ($P < 0.05$) for nine 30-year periods as compared to the historical period under both RCP scenarios (Fig. 9a and c). An average of ~242.4 and 365.0 mm for RCP4.5 and 8.5 scenarios, respectively, was found for the Nebraska site and 569.5 and 855.7 mm for the Texas site ($P < 0.05$). The water yield for the Kansas site also increased significantly under both RCP scenarios. However, the water yield increase in the Kansas site was markedly less than those for the Nebraska and Texas sites averaging ~30.4 and 32.7 mm for the RCP4.5 and 8.5 scenarios, respectively. The changing trend over time in water yield of all sites was not significant except for the Nebraska site under the RCP8.5 scenario ($P < 0.05$) (Fig. 9).

3.4.4. Corn yield response

Overall, predicted average crop yield for the nine 30-year periods was less than the historical period for all three sites under both RCP scenarios ($P < 0.05$; Fig. 10). Average reductions over the entire study period of ~27.3% and 63.7% for the RCP4.5 and 8.5, respectively, were found for the Nebraska site, 30.8% and 68.2% for the Kansas site, and 22.5% and 62.3% for the Texas site. The overall trend in yield over time under the RCP4.5 scenario was relatively stable for the Nebraska and Kansas sites and increased significantly for the Texas site. However, under the RCP8.5 scenario, the trend in yield significantly decreased in a logarithmic form across all sites (Fig. 10).

3.5. Regional differences in simulated ET_c, irrigation, water yield, and crop yield using dynamic input method across various climatic locations

For the RCP4.5 scenario, there was a significant difference ($P < 0.05$) in the average ET_c from 2031 to 2298 across locations, with ET_c values of approximately 509.9 mm, 605.5 mm, and 587.4 mm from north to south (Table 4). The average amounts of irrigation significantly differed among the three sites and the future irrigation requirement for corn production was greatest for the Kansas site, at approximately 98.6 mm. Water yield decreased significantly with decreasing latitudes for the Nebraska, Kansas, and Texas sites by approximately 198.1 mm, 172.5 mm, and 78.4 mm, respectively. This demonstrated that Nebraska was more vulnerable to the risk of runoff in the future. However, corn yield was greater for the Nebraska site, at approximately 7.6 Mg ha^{-1}, and significantly larger than the Texas site (Table 4).

Under the RCP8.5 scenario, the regional variations in simulated mean values of ET_c and irrigation were similar to that of the RCP4.5 scenario (Table 4). Both ET_c and irrigation were greatest ($P < 0.05$) for

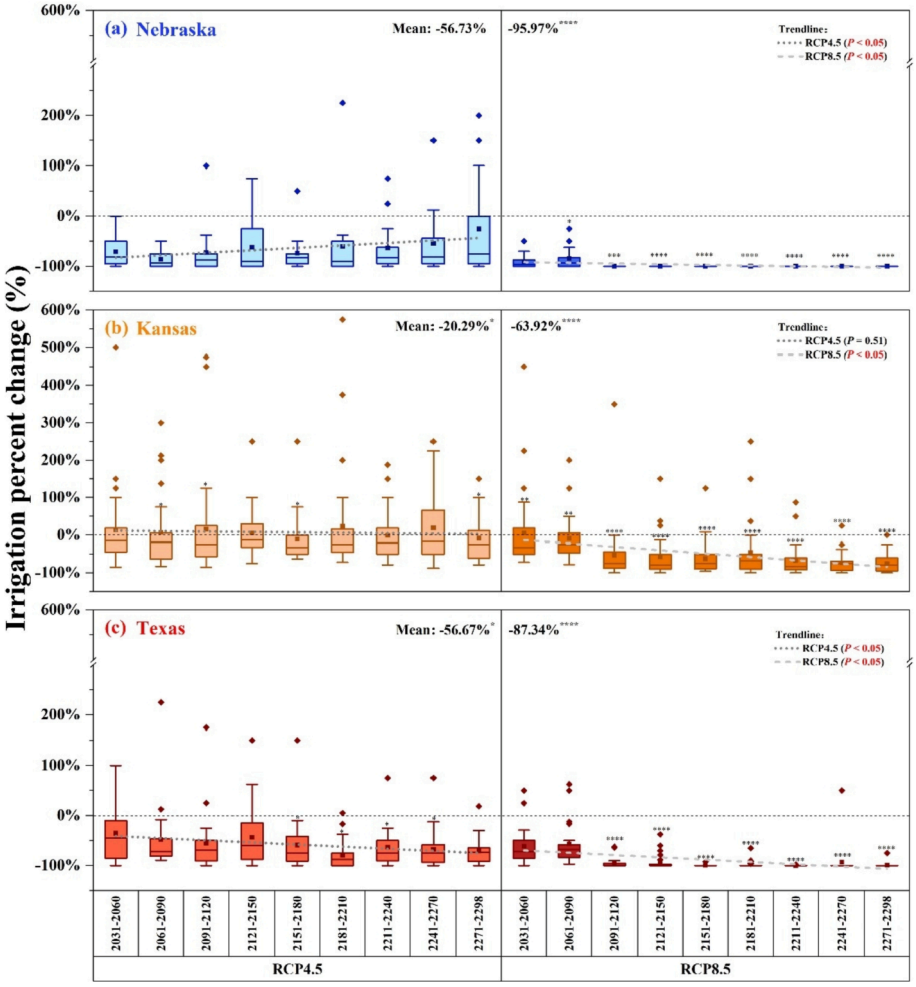

Fig. 8. Box plots showing the simulated annual percent changes in irrigation under RCP4.5 and RCP8.5 scenarios during the 2031–2060, 2061–2090, 2091–2120, 2121–2150, 2151–2180, 2181–2210, 2211–2240, 2241–2270, and 2271–2298 time periods compared to the historical period (1970–1999).

the Kansas site with 478.5 and 44.7 mm, respectively, and lowest for the Nebraska site ($P < 0.05$) (Table 4). Mean values of water yield decreased significantly from north to south with 289.8, 186.4, and 115.9 mm for the Nebraska, Kansas, and Texas sites, respectively. Nevertheless, the simulated mean values of corn yield for the Nebraska site were numerically greater than those for the Kansas site, but no significant difference was found between the two sites. Yield for the Texas site was significantly less than the other two sites and was approximately 3.3 Mg ha^{-1}, thus indicating a noticeable food security issue in Texas in the future (Table 4).

4. Discussion

4.1. *Effects of CO_2 input methods on hydrology and crop yield*

When using the SWAT model to predict and analyze the effects of future climate change on hydrology and crop growth, the CO_2 input in the model was an important influencing factor. The lack of an option for dynamic input of CO_2 concentrations in the current SWAT model limited its efficacy for assessing the impacts of future climate change (Gao et al., 2020; Wang et al., 2017; Zhang et al., 2013). Therefore, this study developed and incorporated a dynamic CO_2 input method into SWAT and compared the differences of major hydrologic variables and corn yields by applying three different CO_2 input methods from 2031 to 2100. Among the three input methods, the default input method simulated the highest ET_c and irrigation continuously, but simulated the least water yield and corn yield (Figs. 2 and 3). Furthermore, the simulated ET_c and irrigation using the dynamic input method were greater than those of the constant input method in the first half of the simulation period and lower in the later period, which highlighted the importance of considering the rising CO_2 levels in the future for water cycling. In contrast, the simulated corn yields using the dynamic input method were less than those using the constant input method in the first half period and greater than those of the constant input method in the second half period generally. Similar results were more evident under the RCP8.5 scenario. These findings emphasized the positive effect of CO_2 on crop yield boost.

It is notable that under the RCP8.5 scenario, the simulated yield for the Texas site was greater for the constant input method relative to the dynamic input method at the beginning of the 21st century. However, by the end of the 21st century, greater yield values were simulated by the dynamic input approach even though the difference was reduced when compared to the constant input method (Fig. 3). This could be explained by the fact that at the beginning of the 21st century, the increase in air temperature was relatively smaller compared to the historical period and there was less temperature stress for corn growth. Yields at this stage were likely more sensitive to the CO_2 fertilizer effect. However, there was a considerable increase in both maximum and minimum air temperatures over time under the RCP8.5 scenario. The limiting effect of temperature stress on corn far exceeded the extent to which yield was positively affected by the elevated CO_2 concentrations at the end of the 21st century. This also explains why corn yields differed less between the dynamic and constant input methods later in the study period.

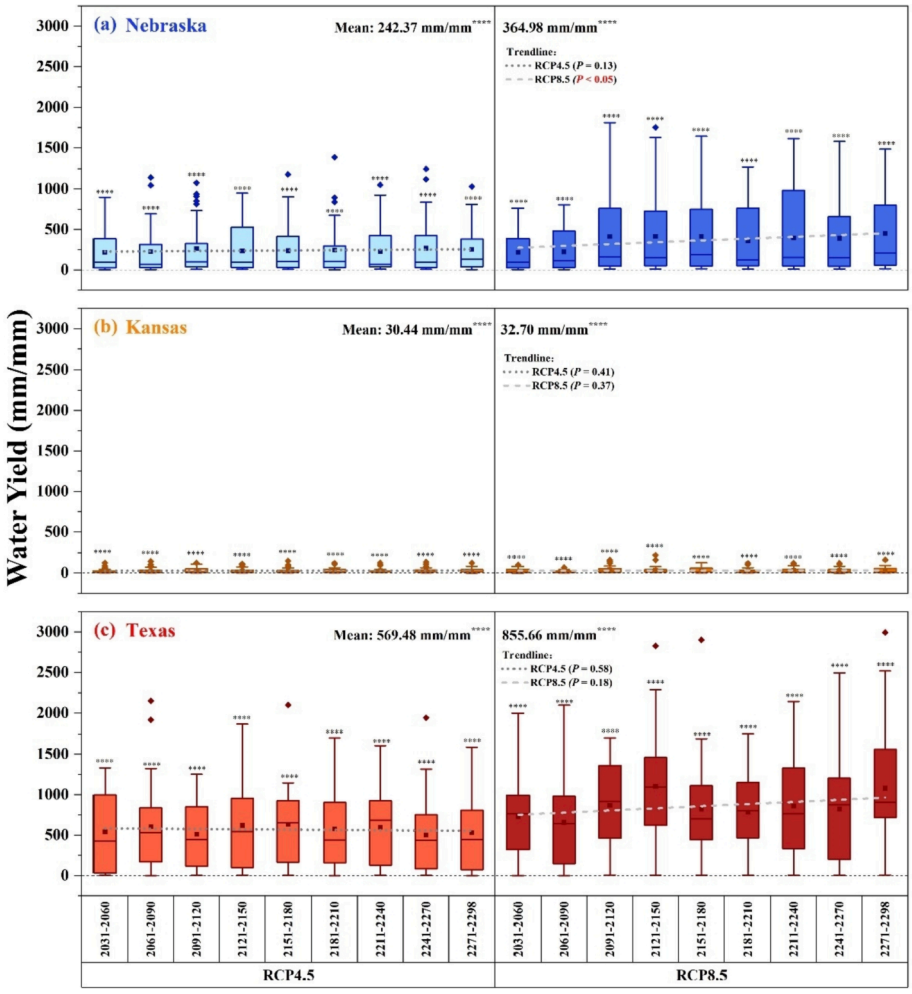

Fig. 9. Box plots showing the simulated annual percent changes in water yield under RCP4.5 and RCP8.5 scenarios during the 2031–2060, 2061–2090, 2091–2120, 2121–2150, 2151–2180, 2181–2210, 2211–2240, 2241–2270, and 2271–2298 time periods compared to the historical period (1970–1999).

Furthermore, the logarithmic rise in air temperatures and logarithmic drop in yields provided evidence for the above explanations (Figs. 5, 6, and 10). Both the constant and dynamic input methods differed significantly from the default input method in simulating hydrologic and yield factors. Therefore, this new method for dynamic CO_2 inputs was necessary for reducing the uncertainty in predicting future climate change impacts compared to previous SWAT studies of no change or using a single input CO_2 value.

4.2. Exploring the causes of future climate change on hydrology and corn yields

In this study, future ET_c, irrigation, and corn yield using the newly developed dynamic input method were predicted to decrease for the Nebraska, Kansas, and Texas sites, with increasing water yield, especially in the RCP8.5 scenario. Under the future climate scenarios, the decreases in ET_c and irrigation were mainly due to the closure of crop stomata and suppression of transpiration caused by the elevated CO_2 concentrations (Bunce and Nasyrov, 2012). For example, Liu et al. (2021) found that stomatal closure and decreased stomatal conductivity negatively affected corn evapotranspiration through a two-year field experiment in Northeast China.

This study showed that changes in future corn yield vary distinctively with geographic locations, such as with the Nebraska, Kansas, and Texas sites from the north to south, which were sequentially lower in latitude by 3° and spanned different climatic locations. This is consistent with other studies showing that spatial and geographic variations could affect crop yields (Asseng et al., 2019; Fletcher et al., 2020; Shin et al., 2017). Under both the RCP4.5 and 8.5 scenarios, corn yield was greater for the Nebraska site and significantly larger than the Texas site ($P < 0.05$). Not only under the future climate, but during the historical period, corn yields from Nebraska were greater than those in Kansas and Texas, which also had lower yields and large yield gaps (Kucharik et al., 2020). Nebraska is abundant in precipitation during the corn growing season with greater humidity, which has a positive impact on corn yields. In contrast, Kansas and Texas are located in the middle and south of the U.S. High Plains and often experience extreme climate conditions such as high temperatures and drought, which are the main reasons for lower corn yields in both regions (Kucharik et al., 2020).

This study predicted reductions in corn yields from the 21st century to the 23rd century under both the RCP4.5 and 8.5 scenarios. Particularly, RCP8.5 suggested crop yield reductions of more than 80% by the end of the 23rd century as compared to the historical period. Many studies have evaluated the impact of climate change on global agricultural systems under the RCP4.5 and 8.5 scenarios and found that crop yields were highly vulnerable to future climate change (Ketiem et al., 2017; Leng, 2018; Tan et al., 2022; Wang et al., 2018). The warming climate can negatively affect corn yield, which is mainly due to greater air temperatures that increase the rate of development and maturation and shorten the growing period of corn (Bassu et al., 2014; Chen et al., 2019b; Wechsung et al., 2021). In this study, the simulated reduction in corn yield was associated with a considerable increase in future air

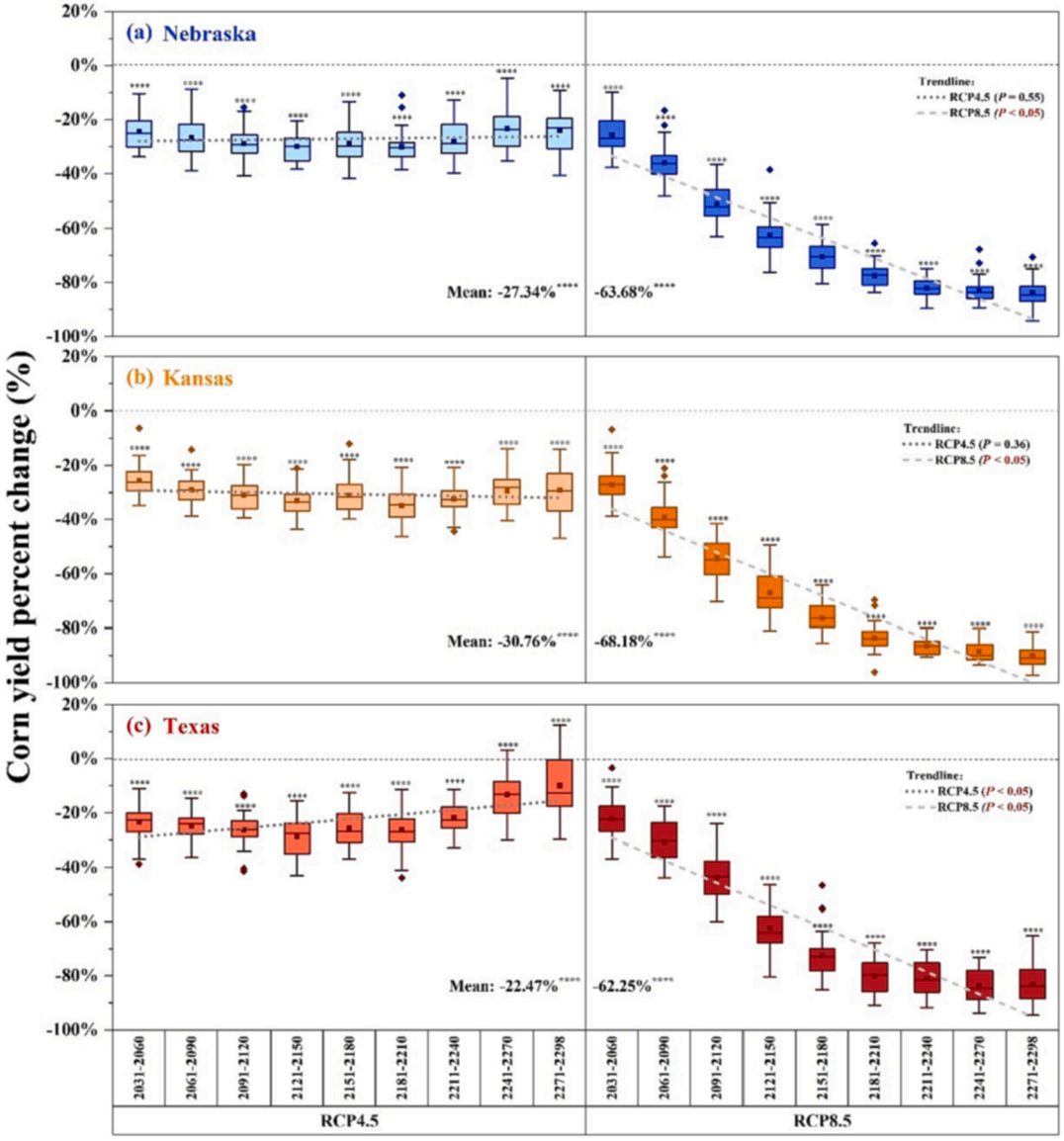

Fig. 10. Box plots showing the simulated annual percent changes in corn yield under RCP4.5 and RCP8.5 scenarios during the 2031–2060, 2061–2090, 2091–2120, 2121–2150, 2151–2180, 2181–2210, 2211–2240, 2241–2270, and 2271–2298 time periods compared to the historical period (1970–1999).

Table 4
Ensemble means of four GCMs for changes in ET_c, irrigation, water yield, and corn yield using dynamic CO_2 input method from 2031 to 2298 across locations (Nebraska, Kansas, and Texas sites).

Scenario/Site		ET_c (mm)	Irrigation (mm)	Water Yield (mm)	Corn Yield (Mg ha^{-1})
RCP4.5	Nebraska	509.87 ± 18.90c	18.60 ± 19.27c	198.12 ± 64.52a	7.56 ± 0.59a
	Kansas	605.51 ± 22.79a	98.57 ± 37.48a	172.45 ± 58.21b	7.63 ± 0.60a
	Texas	587.44 ± 25.93b	45.90 ± 37.72b	78.44 ± 48.31c	6.69 ± 0.72b
RCP8.5	Nebraska	395.18 ± 50.99c	1.75 ± 5.89c	289.78 ± 83.73a	3.79 ± 2.16a
	Kansas	478.49 ± 61.80a	44.71 ± 33.72a	186.43 ± 64.31b	3.52 ± 2.45ab
	Texas	431.56 ± 82.20b	13.48 ± 26.80b	115.94 ± 53.21c	3.28 ± 2.04b

Columns with the same alphabets indicated that the differences were not significant ($P > 0.05$); different alphabets (a, b, and c) indicated that the differences were significant ($P < 0.05$).

temperatures at the study sites. The similar trend of logarithmic increase in air temperatures and logarithmic decrease in yield under the RCP8.5 scenario in this study provided further evidence (Figs. 5, 6, and 10). Few studies have projected climate change impacts on hydrology and crop yield for the next three centuries due to the higher uncertainty associated with longer projections. However, this study is a worthy undertaking to provide valuable insights into long-term climate change impacts on water resources and agriculture sustainability. Using the RCP4.5 and 8.5 scenarios to constrain projections, this study offers possible ranges of what can happen in the future with different feasible mitigation efforts.

5. Conclusions

An improved SWAT model equipped with a dynamic CO_2 input method and a MAD automatic irrigation function was used to explore the influences of future climate change on hydrology and corn yield in the U.S. High Plains. The differences among default, constant, and dynamic input methods under four GCMs of CMIP5 climate data for the RCP4.5 and 8.5 from 2031 to 2100 were investigated in this study. The

results found significantly greater simulated ET_c between the default input method and the other two input methods under the RCP4.5 scenario. The RCP8.5 scenario also exhibited this difference, along with statistically significant differences in ET_c simulations among each of the three input methods for the Nebraska and Kansas sites (default > constant > dynamic). Furthermore, ET_c and irrigation were both increased using the dynamic input method as opposed to the constant input method in the first half of the simulation period and decreased in the second half. This is reasonable when considering that increased CO_2 concentrations induce the partial closing of corn stomata and reduction of ET_c and irrigation requirements. In contrast, simulated corn yield using the dynamic input method was reduced in the first half of the study period and greater in the second half of the period. This highlighted the carbon fertilization effect on corn growth with gradual increases in CO_2 concentrations using the dynamic input method in the future. These findings demonstrated the usefulness of the dynamic input method for SWAT to more representatively predict impact of future climate change.

The dynamic input method was further used to predict changes in hydrology and corn yields under a long-term period from 2031 to 2298 as compared to the historical period of 1970 to 1999. The future period was divided into nine 30-year periods. Both ET_c and irrigation declined the most for the Nebraska site, with ET_c declining by an average of 2.9% (RCP4.5) and 24.7% (RCP8.5) over the entire study period ($P < 0.05$), and irrigation decreased by an average of 56.7% (RCP4.5) and 96.0% (RCP8.5) ($P < 0.05$). ET_c and irrigation were significantly less than the historical period for most of the time periods under the RCP8.5 scenario, and ET_c for the Texas site, and irrigation at all three sites, trended significantly downward under the RCP8.5 scenario. The trendline of water yield was relatively stable over the entire simulation period, but all scenarios and sites were significantly ($P < 0.05$) greater than that of the historical period. Corn yields at all three sites were significantly less than the historical period for different RCP scenarios and periods. Under the RCP8.5 scenario, the trendline of corn yield decreased significantly in a logarithmic form, with crop failure occurring at the end of the 23rd century. The substantially elevated minimum air temperature with the logarithmic form was the major reason for the log decline in corn yield. Overall, the results indicated that the future irrigation, ET_c, and corn yield could decrease at the three sites under different climate change scenarios and could be severe over time. Generally, water yield was increased across different climatic locations under the various climate change scenarios. Thereby, this study is informative and alarming for irrigated corn production in the U.S. High Plains in the context of the severity of the future climate.

Declaration of Competing Interest

The authors declare that they have no known competing financial interests or personal relationships that could have appeared to influence the work reported in this paper.

Data availability

Data will be made available on request.

Acknowledgements

This research was supported in part by the Ogallala Aquifer Program, a consortium between USDA-Agricultural Research Service, Kansas State University, Texas A&M AgriLife Research, Texas A&M AgriLife Extension Service, Texas Tech University, and West Texas A&M University. We greatly appreciate the anonymous reviewers for their valuable comments and suggestions for improving this paper.

Funding

This work was supported by the Chinese Universities Scientific Fund [grant numbers 1191-15051002, 1191-15052008, 1191-10092004, and 1191-31051204]; the National Institute of Food and Agriculture, U.S. Department of Agriculture [grant number NIFA-2021-67019-33684].

References

Arnold, J.G., Srinivasan, R., Muttiah, R.S., Williams, J.R., 1998. Large area hydrologic modeling and assessment part I: model development. Journal of the American Water Resources Association 34 (1), 73–89.

Arnold, J.G., Kiniry, J.R., Srinivasan, R., Williams, J.R., Haney, E.B., Neitsch, S.L., 2011. Soil and water assessment tool input/output file documentation version 2009. Texas Water Resources Institute.

Arnold, J.G., Moriasi, D.N., Gassman, P.W., et al., 2012. SWAT: Model use, calibration, and validation. Transactions of the ASABE 55 (4), 1491–1508.

Asseng, S., Martre, P., Maiorano, A., et al., 2019. Climate change impact and adaptation for wheat protein. Global Change Biology 25 (1), 155–173.

Bassu, S., Brisson, N., Durand, J.L., et al., 2014. How do various maize crop models vary in their responses to climate change factors? Global Change Biology 20 (7), 2301–2320.

Bunce, J.A., Nasyrov, M., 2012. A new method of applying a controlled soil water stress, and its effect on the growth of cotton and soybean seedlings at ambient and elevated carbon dioxide. Environmental and Experimental Botany 77, 165–169.

Butcher, J.B., Johnson, T.E., Nover, D., Sarkar, S., 2014. Incorporating the effects of increased atmospheric CO_2 in watershed model projections of climate change impacts. Journal of Hydrology 513, 322–334.

Callison, D., 2012. Management Allowed Depletion Irrigation Scheduling. Available online at http://awqa.org/wp-content/toolkits/IrrigationScheduling/ManagementAllowedDepletion-IrrigationScheduling.pdf (accessed on 15 July 2022).

Chen, Y., Marek, G.W., Marek, T.H., Brauer, D.K., Srinivasan, R., 2018. Improving SWAT auto-irrigation functions for simulating agricultural irrigation management using long-term lysimeter field data. Environmental Modelling & Software 99, 25–38.

Chen, Y., Marek, G.W., Marek, T.H., Gowda, P.H., Xue, Q., Moorhead, J.E., Brauer, D.K., Srinivasan, R., Heflin, K.R., 2019a. Multisite evaluation of an improved SWAT irrigation scheduling algorithm for corn (*Zea mays* L.) production in the U.S. Southern Great Plains. Environmental Modelling & Software 118, 23–34.

Chen, Y., Marek, G.W., Marek, T.H., Moorhead, J.E., Heflin, K.R., Brauer, D.K., Gowda, P.H., Srinivasan, R., 2019b. Simulating the impacts of climate change on hydrology and crop production in the Northern High Plains of Texas using an improved SWAT model. Agricultural Water Management 221, 13–24.

Chen, Y., Marek, G.W., Marek, T.H., Porter, D.O., Brauer, D.K., Srinivasan, R., 2021. Modeling climate change impacts on blue, green, and grey water footprints and crop yields in the Texas High Plains, USA. Agricultural and Forest Meteorology 310, 108649.

El-Shehawy, R., Gorokhova, E., Fernández-Piñas, F., del Campo, F.F., 2012. Global warming and hepatotoxin production by cyanobacteria: What can we learn from experiments? Water Research 46 (5), 1420–1429.

Evett, S.R., Schwartz, R.C., Mazahrih, N.T., Jitan, M.A., Shaqir, I.M., 2011. Soil water sensors for irrigation scheduling: Can they deliver a management allowed depletion? Acta Horticulturae 888, 231–237.

Feng, S., Hao, Z., Zhang, X., Hao, F., 2021. Changes in climate-crop yield relationships affect risks of crop yield reduction. Agricultural and Forest Meteorology 304–305, 108401.

Fletcher, A.L., Chen, C., Ota, N., Lawes, R.A., Oliver, Y.M., 2020. Has historic climate change affected the spatial distribution of water-limited wheat yield across Western Australia? Climatic Change 159 (3), 347–364.

Gao, X., Ouyang, W., Lin, C., Wang, K., Hao, F., Hao, X., Lian, Z., 2020. Considering atmospheric N_2O dynamic in SWAT model avoids the overestimation of N_2O emissions in river networks. Water Research 174, 115624.

Gupta, H.V., Sorooshian, S., Yapo, P.O., 1999. Status of automatic calibration for hydrologic models: Comparison with multilevel expert calibration. Journal of Hydrologic Engineering 4 (2), 135–143.

Hargreaves, G.H., Samani, Z.A., 1985. Reference crop evapotranspiration from temperature. Applied Engineering in Agriculture 1 (2), 96–99.

Ketiem, P., Makenzi, P.M., Maranga, E.K., Omondi, P.A., 2017. Integration of climate change information into drylands crop production practices for enhanced food security: a case study of Lower Tana Basin in Kenya. African Journal of Agricultural Research 12 (20), 1763–1771.

Kucharik, C.J., Ramiadantsoa, T., Zhang, J., Ives, A.R., 2020. Spatiotemporal trends in crop yields, yield variability, and yield gaps across the USA. Crop Science 60 (4), 2085–2101.

Legates, D.R., McCabe Jr., G.J., 1999. Evaluating the use of "goodness-of-fit" Measures in hydrologic and hydroclimatic model validation. Water Resources Research 35 (1), 233–241.

Leng, G., 2018. Keeping global warming within 1.5 degrees C reduces future risk of yield loss in the United States: A probabilistic modeling approach. Science of the Total Environment 644, 52–59.

Lewis, S.C., King, A.D., Perkins-Kirkpatrick, S.E., Mitchell, D.M., 2019. Regional hotspots of temperature extremes under 1.5 degrees C and 2 degrees C of global mean warming. Weather and Climate. Extremes 26, 100233.
Liu, H., Gao, Z., Zhang, L., Liu, Y., 2021. Stomatal conductivity, canopy temperature and evapotranspiration of maize (*Zea mays* L.) to water stress in Northeast China. International Journal of Agricultural and Biological. Engineering 14 (2), 112–119.
Marek, T.H., Porter D.O., Kenny N.P., Gowda P.H., Howell T.A. Moorhead J.E., 2011. Educational enhancements to the Texas High Plains Evapotranspiration (ET) Network. Technical Report for Contract #0903580956 to the Texas Water Development Board, Austin, Texas. Texas A&M AgriLife Research, Amarillo, Texas. AREC publication 2011-8. 34p.
Marras, P.A., Lima, D.C.A., Soares, P.M.M., Cardoso, R.M., Medas, D., Dore, E., De Giudici, G., 2021. Future precipitation in a Mediterranean island and streamflow changes for a small basin using EURO-CORDEX regional climate simulations and the SWAT model. Journal of Hydrology 603, 127025.
Melaku, N.D., Wang, J., Meshesha, T.W., 2022. Modeling the dynamics of carbon dioxide emission and ecosystem exchange using a modified SWAT hydrologic model in cold wetlands. Water 14 (9), 1458.
Merriam, J.L., 1966. A management control concept for determining the economical depth and frequency of irrigation. Transactions of the ASAE 9, 492–498.
Mishra, S.K., Singh, V.P., 2013. Soil conservation service curve number (SCS-CN) methodology. Springer, Netherlands.
Monteith, J.L., 1965. Evaporation and environment. Symposia of the Society for Experimental Biology 19, 205–234.
Nash, J.E., Sutcliffe, J.V., 1970. River flow forecasting through conceptual models part I – A discussion of principles. Journal of Hydrology 10 (3), 282–290.
National Agricultural Statistics Service (NASS), 2021. Available online: https://www.nass.usda.gov/(accessed on 26 February 2022).
Neitsch, S.L., Arnold, J.G., Kiniry, J.R., Williams, J.R., 2011. Soil and Water Assessment Tool Theoretical Documentation Version 2009. Texas Water Resources Institute.
Pan, S., Chen, G., Ren, W., Dangal, S.R.S., Banger, K., Yang, J., Tao, B., Tian, H., 2018. Responses of global terrestrial water use efficiency to climate change and rising atmospheric CO_2 concentration in the twenty-first century. International Journal of Digital Earth 11 (6), 558–582.
Payero, J.O., Tarkalson, D.D., Irmak, S., Davison, D., Petersen, J.L., 2008. Effect of irrigation amounts applied with subsurface drip irrigation on corn evapotranspiration, yield, water use efficiency, and dry matter production in a semiarid climate. Agricultural Water Management 95, 895–908.
Peel, M.C., Finlayson, B.L., McMahon, T.A., 2007. Updated world map of the Köppen-Geiger climate classification. Hydrology and Earth System Sciences 11 (5), 1633–1644.
Priestley, C.H.B., Taylor, R.J., 1972. On the assessment of surface heat flux and evaporation using large-scale parameters. Monthly Weather Review 100 (2), 81–92.
Qi, J., Zhang, X., Lee, S., Wu, Y., Moglen, G.E., McCarty, G.W., 2020. Modeling sediment diagenesis processes on riverbed to better quantify aquatic carbon fluxes and stocks in a small watershed of the Mid-Atlantic region. Carbon Balance and Management 15, 13.
Qian, S., Kennen, J.G., May, J., Freeman, M.C., Cuffney, T.F., 2021. Evaluating the impact of watershed development and climate change on stream ecosystems: A Bayesian network modeling approach. Water Research 205, 117685.
Rogelj, J., Meinshausen, M., Knutti, R., 2012. Global warming under old and new scenarios using IPCC climate sensitivity range estimates. Nature Climate Change 2 (4), 248–253.
Rudnick, D.R., Irmak, S., West, C., et al., 2019. Deficit irrigation management of maize in the High Plains aquifer region: A review. Journal of the American Water Resources Association 55 (1), 38–55.
Sharpley, A.N., Williams, J.R., 1990. EPIC-erosion/productivity impact calculator: 1. Model documentation. U.S. Department of Agriculture Technical Bulletin.
Sheffield, J., Barrett, A., Colle, B., et al., 2013. North American climate in CMIP5 experiments. Part I: Evaluation of historical simulations of continental and regional climatology. Journal of Climate 26 (23), 9209–9245.
Shin, Y., Lee, E.J., Im, E.S., Jung, I.W., 2017. Spatially distinct response of rice yield to autonomous adaptation under the CMIP5 multi-model projections. Asia-Pacific Journal of Atmospheric Sciences 53 (1), 21–30.
Sloan, P.G., Moore, I.D., 1984. Modeling subsurface stormflow on steeply sloping forested watersheds. Water Resources Research 20 (12), 1815–1822.
Soil Survey Staff, 2010. Keys to Soil Taxonomy, 11th Edition. USDA-Natural Resources Conservation Service, Washington DC.
Tan, L., Feng, P., Li, B., Huang, F., Liu, D.L., Ren, P., Liu, H., Srinivasan, R., Chen, Y., 2022. Climate change impacts on crop water productivity and net groundwater use under a double-cropping system with intensive irrigation in the Haihe River Basin. China. Agricultural Water Management 266, 107560.
Tan, M.L., Gassman, P.W., Yang, X., Haywood, J., 2020. A review of SWAT applications, performance and future needs for simulation of hydro-climatic extremes. Advances in Water Resources 143, 103662.
United Nations Framework Convention on Climate, C., 2015. "Adoption of the Paris Agreement, 21st Conference of the Parties," United Nations.
U.S. Department of Agriculture – Natural Resources Conservation Service (USDA-NRCS), 2017. https://www.nrcs.usda.gov/Internet/FSE_DOCUMENTS/nrcs141p2_017640.pdf (accessed on 15 July 2022).
van Vuuren, D.P., Edmonds, J., Kainuma, M., et al., 2011. The representative concentration pathways: an overview. Climatic Change 109 (1–2), 5–31.
Wang, R., Bowling, L.C., Cherkauer, K.A., Cibin, R., Her, Y., Chaubey, I., 2017. Biophysical and hydrological effects of future climate change including trends in CO_2, in the St. Joseph River watershed. Eastern Corn Belt. Agricultural Water Management 180, 280–296.
Wang, B., Liu, D., O'Leary, G.J., et al., 2018. Australian wheat production expected to decrease by the late 21st century. Global Change Biology 24 (6), 2403–2415.
Wang, Q., Qi, J., Li, J., Cole, J., Waldhoff, S.T., Zhang, X., 2020. Nitrate loading projection is sensitive to freeze-thaw cycle representation. Water Research 186, 116355.
Wechsung, F., Ritter, M., Wall, G.W., 2021. The upper homeostatic range for the temperature-yield response of irrigated US wheat down revised from a theoretical and experimental perspective. Agricultural and Forest Meteorology 307, 108478.
Wu, Y., Liu, S., Abdul-Aziz, O.I., 2012a. Hydrological effects of the increased CO_2 and climate change in the Upper Mississippi River Basin using a modified SWAT. Climatic Change 110 (3), 977–1003.
Wu, Y., Liu, S., Gallant, A.L., 2012b. Predicting impacts of increased CO_2 and climate change on the water cycle and water quality in the semiarid James River Basin of the Midwestern USA. Science of the Total Environment 430, 150–160.
Yuan, S., Quiring, S.M., Kalcic, M.M., Apostel, A.M., Evenson, G.R., Kujawa, H.A., 2020. Optimizing climate model selection for hydrological modeling: A case study in the Maumee River basin using the SWAT. Journal of Hydrology 588, 125064.
Zhang, X., Izaurralde, R.C., Arnold, J.G., Williams, J.R., Srinivasan, R., 2013. Modifying the Soil and Water Assessment Tool to simulate cropland carbon flux: Model development and initial evaluation. Science of the Total Environment 463–464, 810–822.
Zhang, Q., Shen, Z., Xu, C.Y., Sun, P., Hu, P., He, C., 2019. A new statistical downscaling approach for global evaluation of the CMIP5 precipitation outputs: Model development and application. Science of the Total Environment 690, 1048–1067.